VOLUME 2, 2018
DOI: 10.31058/j.am.2018.23001

Bioceramics: Materials, Properties and Applications-Part III

Hassan H. M. Darweesh[1*]

[1] Refractories, Ceramics and Building Materials Department, National Research Center, Dokki, Cairo, Egypt

Email Address

hassandarweesh2000@yahoo.com (Hassan H. M. Darweesh)
*Correspondence: hassandarweesh2000@yahoo.com

Received: 24 December 2017**; Accepted:** 7 February 2018**; Published:** 13 August 2018

Abstract:

The up to date or recent field of nanotechnology is considered as one of the most exciting and promising science branch so that it deals with all science branches particularly biology, medicine, tissue engineering, bone scaffolds, cement and bioceramic industries in which biomaterials could be used as bone scaffolds in the human bodies. The author interests with using the nano- and biomaterials to prepare the ceramic batches containing ultrafine and nano-raw materials to indicate the importance of nanomaterials and/or nanoparticles for improving the physicochemical and mechanical properties and microstructure of the resulting bioproducts. This can help people whom are suffering from the deficiency in their body bones as a result of accidents. These bioceramic products can compensate people for their lost or broken bones, as arms, legs, fingers or even toes.

Keywords:

Nanoparticles, Biomaterials, Ceramics, Bioceramic, Bone Scaffolds

1. Introduction

There is an advanced branch of ceramics known as “Bioceramics” including the ceramic products which can be used mainly inside the human bodies as bioactive bone scaffolds. Calcium phosphate-based on bioceramics have received a considerable attention as bone—graft substitutes because of their excellent biocompatility, bioactivity and osteoconductive characteristics compared to other materials. One of these bioceramics is hydroxyapatite (HA) which has a similar chemical composition to the major inorganic component of the skeletal tissue of vertebrates. The graft challenge facing the use of ceramics in the human body is to replace the old deteriorating bone with a material that can function the remaining years of the patient’s life because the average life span of the human beings is about 80 years or may be little more. Moreover, the need for spare parts starts at about 60 years old and the bioceramic parts need to last for 20 years. The bones in the skeleton are not all solid. The outside (cronical bone) is the solid part of the bone with few small canals. The inside of the bone (trabecular bone) likes scaffolding or a honey-comb (Figure 1). The spaces between the bones are filled with fluid bone narrow cells which are making the blood and some fat cells. Figure 2 shows a simple structure of the bone.

Bones with a variety of shapes and sizes and have complex internal and external structures tissues. The most widely ceramic bioactive materials are alumina (Al_2O_3) and zirconia (ZrO_2) due to their excellent biocompatibility. The main advantages of Al_2O_2 are its high hardness and wear resistance while ZrO_2 exhibits higher strength and fracture toughness in addition to the lower Young's modulus [1-7].

Figure 1. *The outside (cortical) and Inside (trabecular) of a bone.*

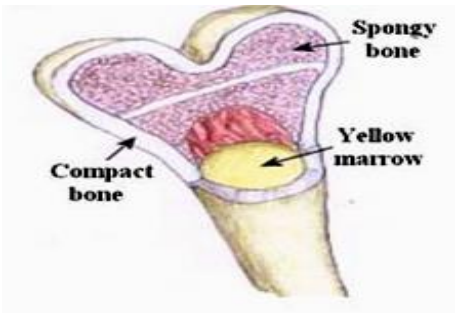

Figure 2. *A simple structure of a bone.*

The sol-gel derived porous alumina and zirconia toughened alumina (ZTA) substrates can be prepared and impregnated with synthetic body fluid (SBF) and dicalcium phosphate (DCP) solutions for different periods to prepare the bioactive composites [8-12]. The resulting porous ceramic substrates are then characterized by measuring their physical properties in terms of bulk density and apparent porosity. The phase composition and the microstructure of the prepared scaffolds or porous ceramic substrates can be determined by using XRD and SEM techniques [2,13,14]. Some investigators [15-21] used a certain polymer based on the getatin from bovine skin (Figure 3) and agarose (Figure 4) to prepare composite scaffolds using the sol-gel technique. They also used the ciprofloxacin of concentration 2 mh/ml (Figure 5) to avoid bacterial infections [22-24].

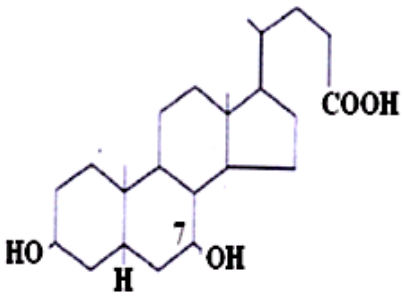

Figure 3. *Chemical structure of Gelatin.*

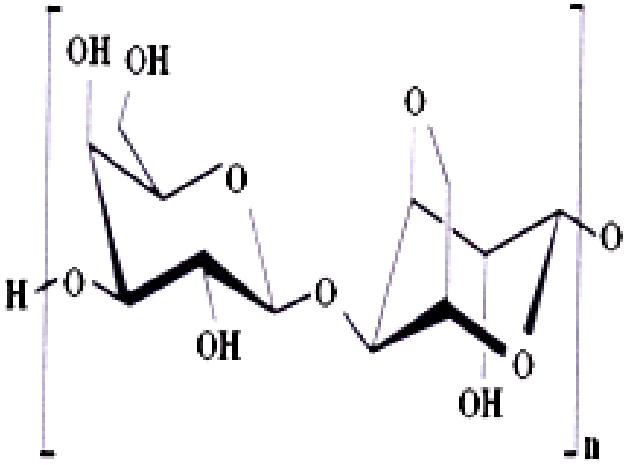

Figure 4. *Chemical structure of Agarose.*

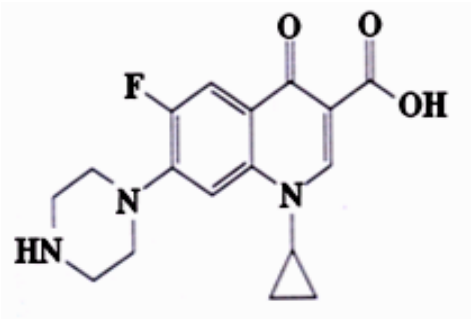

Figure 5. *Chemical structure of ciprofloxacin.*

A biologically promising material with improved mechanical property has been developed, where the graphene oxide of varying amount were incorporated into a gelatin-nanobioactive glass (nBG-Gel) matrix through a freeze drying process. The compressive strength was carried out to determine the reinforcement effect of GO and it demonstrated that nBG-Gel matrix with GO shows a higher compressive strength and a compressive modulus than those of the bare. The porous structure of the composite scaffolds in terms of pore size and pore interconnectivity were tested. The morphological characterization revealed the formation of an interconnected porous hybrid of size range of 100 to 600 μm. The thermal properties of the hybrid were analyzed by Simultaneous Thermal Analyzer (STA). The experimental results demonstrated that the prepared hybrid scaffolds are a potential candidate for the bone tissue engineering [12].

2. The Sol-Gel Technique Of Bioceramics

The sol–gel process is a chemical synthesis technique for the preparation of glasses and ceramics (Figure 6). The chemistry involved in the process is based on inorganic polymerization reactions of metal alkoxide precursors M(OR)*n*, where M represents the network forming element such as Si and R is an alkyl group C*x*H2*x*+1. These precursors undergo hydrolysis and condensation reactions, usually when dissolved in a solvent, to form soluble metal hydroxides, which ultimately leads to the formation of continuous metal–oxygen–metal link as in an inorganic network that spans throughout the solvent medium [2,25,26].

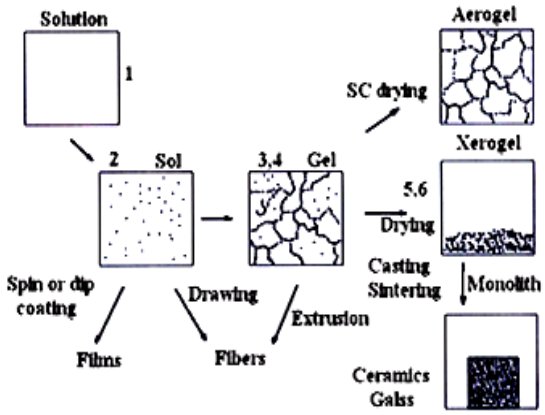

Figure 6. *The sol-gel preparation technique 1-Hydrolysis, 2: Condensation, 3: Gelation, 4: Ageing, 5: Drying and 6: Densification.*

The main features of the multi-component sol–gel process are that a homogeneous solution is formed before polymerization occurs and the processing takes place at lower temperatures than in conventional methods. Thus, not only can improved chemical homogeneity be achieved with good control over the final composition and tailoring of the surface characteristics of the product but also phase separation, crystallization and chemical decomposition can be avoided [27]. Briefly the major advantages associated with the Sol-gel processes include lower processing temperatures, high levels of purity, control of concentrations, and the ability to synthesize multicomponent compositions in different product forms [28]. In addition to Sol–gel derived bioactive glasses tend to have more simple compositions than the melt-derived bioactive glasses and exhibit enhanced bioactivity and resorbability, due to the mesoporous texture (pore diameters in the range 2–50 nm) inherent to the sol–gel process [29]. Also it is believed that enhanced bioactivity can be achieved in gel-derived materials because of their residual hydroxyl ions and micro pores, and a large specific surface area [30,31]. For these reasons sol-gel process in the present study was used. The dynamics of the sol–gel processes are dependent on various physical and chemical properties of the composition of the sol–gel, viz. water to precursor ratio, type of catalyst, choice of precursors, pH, temperature and solvent [32].

3. Properties and Application

$CaSiO_3$ powders for the present studies were synthesized by Sol–gel process, with compositions of 51.72 wt% SiO_2 and 48.28 wt % CaO by the reaction of tetraethyl orthosilicate, and calcium nitrate tetrahydrate. tetraethyl orthosilicate was used as metal alkoxide precursors of the corresponding oxide SiO_2, where many metal alkoxides, especially those that are liquids, can be obtained in exceptionally high levels of purity (99 %, metals, basis). This purity, combined with the volatile nature of certain metal alkoxides, enables these precursors to be used not only in the Sol-gel process but also in processes such as chemical vapor deposition (CVD). This is one of the reasons that metal alkoxides represent the precursors of choice for gel processing of oxide ceramics and glasses [28]. calcium nitrate tetrahydrate [$Ca(NO_3)_2$ 4H2O] was used as the calcium oxide source where unlike the silicon alkoxides, alkoxides of Group I and II metals are usually solid, non-volatile and have very low solubility. Metal salts provide a viable alternative and are usually in the form of nitrates as they are less thermally stable compared to chlorides or sulphates and the anion is relatively easier to remove by decomposition. Although acetate salts can also be used, they do not thermally degrade cleanly and thus leave carbonaceous residues. Also acetate

solutions are basic (high pH) and therefore lead to rapid gelation in silicate systems [27]. Calcium carbonate did not also used where the co-existence of $CaCO_3$ in the amorphous-CS may be disadvantage point for biomedical application because it is considered to show negative effect in vivo [33]. Carbonate ions incorporated in the hydrated layer slow down the development of the apatitic domain (carbonate ions are known as apatite crystal growth inhibitors) [34]. In addition to Calcium nitrate tetrahydrate salt when is used as the calcium precursor eliminating the need for careful hydrolysis as required with metal alkoxides where In practice, differential hydrolysis and polycondensation rates of different alkoxides pose a problem [35]. So calcium metal was introduced in the present study in the form of calcium nitrate tetrahydrate. These were the reasons that metal alkoxides and calcium nitrate represent the precursors of choice for gel processing of oxide ceramics and glasses. Compositions of 51.72 wt % SiO_2 and 48.28 wt % CaO was used because this composition represent the stoichiometric composition of $CaSiO_3$, hence pure wollastonite without additional phases was obtained. This explains the cause for choice TEOS and calcium nitrate tetrahydrate as starting materials and as well as the percentage of them to prepare wollastonite in the present study.

The rate of hydrolysis of TEOS is slow in neutral solutions [27,36] so nitric acid (HNO3) was used to catalyze the TEOS hydrolysis during the sol preparation. Use of an acid catalyst allows for the protonation of the OR groups allowing the hydrolysis of all these groups, an outcome which may not be possible in neutral conditions due to the partial charge distribution in partially hydrolyzed alkoxides [37]. The choice for using HNO3 was depending on using it by several investigators [16,27,28,38-44]. In the present study the procedure was carried out also without catalyst and this lead to delay in hydrolysis and condensation of TEOS and gelling time to produce powder. The powder was obtained after 7 days instead of 10 hr in case of the use of HNO3 as catalyst. Meiszterics and Sink′o [31] reported that the gelling time of the precursor solutions and obtaining the powder depends on the kind of catalyst and it is not possible to obtain any gel system without the presence of water and catalyst, in addition to the porosity of gel samples prepared with catalyst depends strongly on the water content of the initial gelling solutions From a diluted system, a porous gel forms, the concentrated solutions turns into a more compact gel system. Also concluded that the presence of water, without any catalysis results in elastic homogeneous gel structures, on the other hand these gels need a long drying time and this was in a good agreement with our results. While, Bansal reported that a clear transparent gel was obtained in less than an hour to several days depending on the reaction temperature, water concentration and calcium content [27,45,46,47]. On the other hand, Brinker and Scherer [40] considered that gelation in sol–gel is strongly dependent on H_2O/TEOS ratios and at lower ratios the gelation time has been reported to be faster.

Water acts as the “initiator” and is usually externally added. Water can also be generated *in situ* by condensation reactions such as the formation of esters by the condensation of carboxylic acids and alcohols [4]. In some researches, ethyl alcohol could be used as a solvent, Since most alkoxides are insoluble in or immiscible with water, the hydrolysis of an alkoxide occurs upon adding water to a non-aqueous solution (e.g., alcohol) of the alkoxide, whilst Saravanapavan and Hench [27] reported that the CaO content is always lower than that of the theoretical value, the variation is within 25 % and attributed the variation to the leaching of cations during the aging and drying stages when the process is carried out in the presence of the pore liquor (ethyl alcohol). In the present study ethyl alcohol did not used.

After a transparent green sol was obtained, The sol was held at 60 ˚C (aged) to reach high viscosity near the gel point where transparent gel was formed (in the present procedure two hours at 60˚C, the gelation began. This temperature was in agreement with other research [26,27,38,41,42,43,44,45,46,47,48], and in the present study was chosen on the basis of observation of temperature at which the solution become completely miscible or in other word when the solution become completely miscible the temperature already reach to 60 ˚C so we kept the solution at this temperature to obtain transparent gel system. During this aging or pre-polymerization stage, hydrolysis and condensation continues and this results in an increase in viscosity [49,50]. Saravanapavan and Hench [23] demonstrated that the gel point (tgel) varied between 24 h for high Ca gels (0.5–0.3 mole fraction Ca) and 36 h for low Ca gels ($S_{80}C_{20}$ and $S_{90}C_{10}$ samples). The reduction in gelling time with increasing Ca^{2+} content is thought to be due to the lowering of ionic charge on sol particles by the salt. And at the end of the aging period shrinkage of the gels was on average found to be 10–20 % of the original size, depending on size and composition of the original gel. Smaller gels with higher Ca^{2+} content had higher % shrinkage [27]. Gupta et al. [28] reported that the gelation leads to increase in viscosity, shrinkage in volume, loss of weight and decrease in pore size. Scherer [51] also reported that Chemical reactions continue after the gelation, leading to increasing rigidity and, in some cases, to spontaneous shrinkage called “syneresis”. After that the drying of the gel was carried out in stages by raising the temperature to 110 ˚C slowly. Where, the transparent gel dried to remove water and physically adsorbed molecules such as moisture from the pores. Drying and heat treatment will then progressively densify the gel by elimination of water. During the drying process the discs transformed from transparent to translucent /opaque. The drying process yields a powder-like product. Drying of the gel was carried out in stages by raising the temperature 110 ˚C slowly in order to avoid cracking. Viitala et al [52] reported that drying stage is very important if homogeneous, crack-free materials are desired. Especially for monoliths the drying has to be slow in order to avoid cracking.

Crayston [32] reported that the method of drying then determines the nature of the final product: the gel can either be heated to drive off the trapped solvent molecules leading to capillary pressure and a collapse of the gel network; or, alternatively, the gel may be dried supercritically, which allows solvent removal without network collapse. The final product obtained from supercritical drying is called an aerogel that from heating is called a xerogel. Drying and heat treatment will then progressively densify the gel by elimination of water.

Scherer [51] reported that during drying, capillary pressure on the order of 10 to 100MPa develops and produces huge shrinkage of compliant gels. As the gel shrinks, its modulus increases by several orders of magnitude; shrinkage stops when the network is stiff enough to resist the capillary forces. Warping and cracking do not depend on the magnitude of the capillary pressure, but only on the gradient in pressure within the body. Slow drying reduces the gradients and prevents damage.

Saravanapavan and Hench [23] noted that lower Ca^{2+} content gels were white in colour (S90C10 samples) whereas the other compositions ranged from light yellow (S80C20 and S70C30 samples) to yellow (S60C40 and S50C50). This was due to the increasing nitrate content in the gels. When the wet-gels were exposed to the atmosphere the discoloration was stronger. In the present study light yellow was obtained.

After the drying process, the gel networks were converted to white powder. The dried gels were calcined at 500, 600 and 800˚C for 2 h with a heating rate of 5 ˚C min-1. The object of this step is to eliminate organic content and achieve nitrate removal and further densification. Calcination temperature 800˚C gives no weigh loss therefore complete elimination of nitrate and the calculated amount of wollastonite was obtained. The holding time was 2hr. calcination time may have provided sufficient time to establish additional nucleation sites before crystal growth in glass powders.

Wollastonite powder was calcined at 500 ˚C in some researches [29,49,50], other researches calcined wollastonite at 600 ˚C [51-53] and other research calcined wollastonite at 700 ˚C [34,54,55], in addition to some researches [51,55,56] which calcined it at 800 ˚C. The holding time used in this study for calcination was used by some researches [29,42,48,49,54-57].

Saravanapavan and Hench [23] noted that by DTA/TGA curve for a wet S50C50 gel sample, There is an initial endothermic process around 100 ˚C which can be attributed to loss of residual water and ethanol (i.e. pore liquor) corresponding to approximately 25 % reduction in weight. This weight loss is more gradual and occurs over a range of temperatures up to 450 ˚C. This is attributed to the loss of organics (i.e. alkoxy group) after the loss of pore liquor. A second endothermic process occurs at around 550 ˚C with a weight loss of 35 % attributed to the loss of nitrates used in the sol preparation. No weight loss was observed after this temperature and also reported that gel-glasses produced are confirmed to be amorphous even after stabilization at 600 ˚C, with crystallization temperatures above 850 ˚C.

Alemany et al [33] found that from the TG curve there was a weight loss of 14% is observed between room temperature and 150 ˚C. A second weight loss of 54% occurs from 150 ˚C to 600 ˚C. Then the weight remains almost constant up to 1350 ˚C. In the DTA curve, four endothermic peaks at 150 ˚C, 570 ˚C, 560 ˚C and 1200 ˚C as well as one small exothermic at 900 ˚C, can be observed. The first endothermic process may be attributed to the elimination of humidity from the atmosphere and the residual alcohol in the pores of the gel. The endothermic peaks at 570 ˚C and 560 ˚C may be due to the elimination of the nitrates introduced as calcium nitrate in the preparation of sol. While Duval indicated that calcium nitrate is stable up to 475 ˚C and from that temperature the NO_2 elimination starts.

Lao et al. [41] heated the powder at 700 ˚C for 24 h to achieve nitrate elimination and further densification. Liu and Miao [43] reported that at 800 ˚C, only a broad peak existed in the pattern, showing that the bioglass powder 58S still kept the amorphous state. With further increase of the temperature, crystallization occurs. Padilla et al [55] stated that the materials of 70S30C treated at 700 ˚C and 800 ˚C showed XRD patterns typical of amorphous materials. Olmo et al [35] reported that three sol–gel glasses, with SiO_2 as the main constituent (75, 72.5 and 70 mol %), identical CaO content (25 mol %), and without or with P_2O_5 as third constituent (0, 2.5 and 5 mol %) were heated 3 h at 700 ˚C for nitrate removal and stabilization. This stabilization temperature was picked out from the thermogravimetric analysis of the dry powders in a Seiko Thermobalance 320, which showed that the mass remained constant over 700 ˚C for the three compositions. Xia and Chang [39] concluded from the TG curve for CS that there was a gradual mass loss of CS below 821 ˚C.

Meiszterics and Sink′o [31] told that according to the thermo gravimetric analysis (TG curves) the heat treatment of Ca silicate gel systems should be carried out above

600 ˚C. where according to the TG–DTA up to 1000 ˚C, the mass loss of wet gels occurs in two main steps (20–100 ˚C; 530–615 ˚C) in the diluted samples and in three steps (20–100 ˚C; 250–325 ˚C; 500–600 ˚C) in the sample prepared with acetic acid without surplus water, respectively. The weight loss in the first step (20–100 ˚C) can be attributed to the loss of residual water. The second step (250–325 ˚C) belongs to the evaporation of organic compounds after the loss of the pore liquid. The last step can be associated with the escape of nitrate molecules. No weight loss was observed after that. On the basis of TG curves, the heat treatment of Ca silicate gel systems should be carried out at about 600 ˚C. The mass loss reaches more than 90% until 600 ˚C in every sample prepared with acetic acid catalysis.

After the calcinations step, powders were ground and sieved to obtain 63 μm particulates, this particle size was chosen by other researches [35,51,58-60], where range of particle size from 32 to 63 μm. Sieved powder pressed into cylinder with 15 mm in diameter and under different compaction load to obtain the optimum load. A pressure of 60 KN was chosen on the basis of some experiments which will be discussed later. In order to get a hard material, cylindrical specimens of calcium silicate subsequently sintered for 3 h in electric furnace in the range between 900 and 1250 ˚C (heating rate 5 ˚C/min in all cases). The samples were cooled to room temperature in the furnace. As for holding time for sintering Lin et al [57,61] confirmed that the increase of the holding time from 1 to 3 hours resulted in increase in mechanical properties and remain constant with further increase. So, 3hrs were the optimum condition to achieve the best mechanical strength of $CaSiO_3$ ceramics.

Also, other investigators [27,29,44,52,63] chose 3 hrs as holding time and this was the basis for our choice while the sintering temperatures were chosen on the basis of there is no weight loss in the produced powder after 800 ˚C. in addition to from the $CaO–SiO_2$ phase diagram the phase transition temperature of β-$CaSiO_3$ and α-$CaSiO_3$ is 870 ˚C (from amorphous to β-$CaSiO_3$) and 1125 ˚C (from β-CaSiO3 to α-$CaSiO_3$), respectively [44]. Furthermore in the present study X-ray diffraction analysis was carried out in order to determine crystalline phases present at these temperature and be sure that wollastonite is the major phases without any traces of impurities. Finally these range of temperature (900-1300 ˚C) was the range which used by other researches [16,22,24,64-70]. Xia and Chang [39] stated that the DSC showed a sharp exothermic peak at 832 ˚C, which was corresponding to the formation of β-$CaSiO_3$, and a broad exothermic peak at 1142 ˚C, which was corresponding to the formation of α-$CaSiO_3$.

Saravanapavan and Hench [23] reported that gel-glasses produced are confirmed to be amorphous even after stabilization at 600 ˚C, with crystallisation temperatures above 850 ˚C. Padilla et al [55] concluded that in samples 70S30C the crystallized phases were similar when treated at temperatures from 900 ˚C to 1200 ˚C, consisting of a mixture of wollastonite (W) and pseudo-wollastonite (PsW) (polymorphs of $CaSiO_3$), being PsW the majority phase. At 1300 ˚C only PsW and a little amount of cristobalite (Ct, SiO_2) were observed. At this temperature the W-phase was transformed into PsW, which is the most stable phase at high temperature. At 1400 ˚C the Ct content increased significantly.

Arstila et al [65] told that wollastonite type glasses crystallized around 900 ˚C. Liu and Miao [43] reported that at 800 ˚C, only a broad peak existed in the pattern, showing that the bioglass powder still kept the amorphous state. With further increase of the temperature, sharp peaks appeared at 1000 ˚C, indicating crystallization

occurred in the 58S bioglass. The peaks matched the pattern of wollastonite $CaSiO_3$. The $CaSiO_3$ peaks became much sharper at 1200 ˚C, corresponding to further crystallization. Liu, and Ding [66] stated that the sintering temperature did not raised above 1300 where according to the $CaO–SiO_2$ binary system phase diagram, the tridymite, metastable phase of quartz, is easy to precipitate from the wollastonite melt at 1436 ˚C. The tridymite can be retained at room temperature resulting from rapid cooling.

The lower sintering temperature in sol gel process was explained by some research where; Phul é and Wood [24] stated that the transformation of a sol or solution into an essentially inorganic crystalline ceramic or glass, via a gel-like intermediate, can be often accomplished at temperatures that are significantly lower than those necessary in ``traditional" processing. This is because the precursors used are intermixed at a molecular level and can react through chemical pathways to form a network of chemical bonds that are characteristic of completely inorganic materials. Therefore, in sol-gel processing high processing temperatures, used typically to induce long-range diffusion of atoms, are often not needed. Crayston [32] attributed the Lower temperature synthesis to the homogeneity of the dried powder/gel product and the smaller particle size when compared to grind-and-fire methods, nucleation and growth of crystalline phases can occur at lower temperatures. This also allows the synthesis of metastable phases and the inclusion of organic or other compounds with low thermal stability into the final product. While Roy suggested that because of the excess free energy of a gel compared to a glass of the same composition, a gel might be converted to glass at temperatures substantially below the liquidus temperature of that composition [23].

Finally, to tailor the desired properties of silicate glasses, changes in glass composition also were accomplished. Different compositions of sol–gels were prepared by varying the additives (alumina, zirconia and titania) and additive percentage (10, 20 and 40 %). In this work, widely varying compositions, physical, biological and mechanical properties including wear properties were studied in order to provide general information needed to find a proper, optimum condition for material that used as biomaterial and to apply the system in biomedical application [63-66]. Emphasis is placed on the composition dependence of particular species that are ultimately responsible for the enhanced bioactivity of the systems [38].

Bioactive glasses and glass-ceramics (which represent wollastonite in the present study which proposed as potential materials for bone tissue regeneration) is generally not just limited to load-bearing implants. Yet, the use of the latter material could widen their application fields by combining the mechanical properties of this material (Al_2O_3, ZrO_2, TiO_2) which represents a bioinert material with the bioactivity of wollastonite. In fact, the final goal is to combine the bioactive properties with the strength of this inert bioceramic and to propose this biomaterial as implant and dental implants. Materials which used as additives to improve mechanical properties and used it in load bearing bone substitution were chosen due to its high wear resistance, their excellent scratch resistance, good frictional properties and fracture toughness [65-67]. The high stability (low corrosion, low ion release) that characterizes oxide ceramics in the most aggressive conditions is due to the high heat of formation of their molecules in addition to its biocompatibility with the physiological environment, make this ceramic material reliable for a variety of applications, these materials already used in biomedical applications including total hip- and knee-prostheses and

dental implants but as a bioinert material. Hence, ceramic oxides (alumina, Al_2O_3); titania, TiO_2 and zirconia, ZrO_2) have been introduced as reinforcing agents [68-74].

A cellular scaffold materials derived from the extracellular matrices of intact tissues have been successfully used for a variety of tissue engineering and regenerative medicine applications in both preclinical studies and in clinical applications. However, there have been few reports on a cellular rat brain matrix (ARBM) scaffolds and their biocompatibility. In this study, we focused on the compatibility of these scaffolds with neural stem cells in culture applications. The ARBM scaffolds were prepared and cross-linked by genipin and then co-cultured with neural stem cells (NSCs) *in vitro*. The viability the NSCs in the scaffolds was tested using 3-(4,5-dimethylthiazol-2-yl)-2,5-diphenyl tetrazolium (MTT) assay on days 1, 3, 5, and 7. The attachment and growth of the cells in the scaffolds were observed using hematoxylin-eosin (H&E) staining, scanning electron microscopy (SEM), and confocal laser scanning microscope (CLSM). A growth curve indicated no significant difference between cells co-cultured in these scaffolds and in the complete culture medium. The scaffolds showed no cytotoxicity to the NSCs, fostered attachment and proliferation, had steady porous 3D structures, and promoted the axonal growth of NSCs. Thus, these ARBM scaffolds are highly cytocompatible and may be used as cell carriers for the implantation of neural stem cells in the tissue engineering of the central nervous system [75].

4. Conclusions

The nano - and/or biomaterials are recently used to prepare the ceramic batches containing ultrafine or nanoparticles to produce different shapes and sizes of bone scaffolds to place them inside the human body to lighten the pains of patients subjected to traffic accidents and lose a part or more of their body bones. In the future, the scientists must interest to increase and look for new and more effective materials suitable to produce artificial bone scaffolds.

Conflicts of Interest

The author declares that there is no conflict of interest regarding the publication of this article.

References

[1] Taha, R. T. A. Bioceramic composites suitable for bone graft. M. Sc. Thesis (Biophysics), University College of Women, Ain Shams University, 2011.

[2] Mohamed, E. M. Inorganic –organic hybrids based on PVA and Silica with added titania. M. Sc. Thesis (Biophysics), University College of Women, Ain Shams University, 2012.

[3] Kokubo, T. Bioactive glass ceramics" Properties and applications. *Biomaterials*, 1991, 12, 155-163.

[4] Iarry, H. L. Bioceramics from concept to clinical. *Amer. Cer. Soc.*, 1991, 74, 1487-1491.

[5] Klein, l. *Sol-gel optics: Processing and applications*. Springer Verlag, 1994, ISBN 0792394240.

[6] Kong, Y. M.; Kim, S.; Kim, H. E. Reinforcement of hydroxyapatite bioceramics by addition of ZrO2 coated with Al2O3. *Amer. Cer. Soc.* 1999, 82, 2963-2968.

[7] Susan, H. *Basic biomaterials*. 5th Edn. 2007, 88, 0071260412.

[8] Natesan, K.; Shah, W.; Le, H. R.; C. Tredwin, A Critical Comparison on Biocompatibility of Different Phases of Sol-Gel Derived Calcium Phosphates as Bone Graft Materials. *J. Biomater. Tissue Eng*. 2015, 5, 655-664.

[9] Zhu, W.; Cui, J.; Duan, L.; Chen, J.; Zeng, Y. and Wan,g, D. Research Progress of Scaffold Materials in Cartilage Tissue Engineering. *J. Biomater. Tissue Eng*. 2015, 5, 673-679.

[10] Yang, T.; Wang, H.; Zhang, F.; Meng, G.; Chen, Z. and Ren, X. Glucocorticoid Modulated Crystallization of Apatite Nanocrystals. J. Biomater. Tissue Eng. 2015, 5, 697-702.

[11] Hyuck, B.; Ryu, D. H.; Kim, S.B.; Kim, S.B.; Jung, Y.J.; Yoon, l.; Jeon, M.; Shim, Y.K. and Lee, W.K. Fabrication and Evaluation of Scaffolds Using Porous Microparticles and Simplified Microsphere Sintering Method. *J. Biomater. Tissue Eng.* 2015, 5, 722-729.

[12] Samad, S.A.; Arafat, A.A.; Gafur, M.A. and Chowdhury, A.M.S. Characterization of Scaffold Prepared by Blending Nanobioactive Glass and Graphene Oxide Gelatin Hydrogel Solutions for Bone Tissue Engineering. *J. Biomater. Tissue Eng.* 2015, 5, 620-627.

[13] El-Hady, B.I.; El-Kady, A.M.; Hassan, M.M.A. Preparation and characterization of biocomposites for localized bone treatment based on Agarose and Gelatin", Ph. D. Thesis (Biophysics), University College of Women, Ain Shams University, 2015.

[14] Hench, L.L.; West, J.K. The sol-gel process. *Chemical Review*, 1990, 90-133.

[15] Daniel, A.; Vallet-Regi, M. Sol-gel silica based biomaterials and bone tissue regeneration. *Acta Biomaterialia*, 2010, 6, 2874-2888.

[16] Balamurugan, A.; Balossier, G.; Laurent-Maquin, D.; Pina, S.; Rebelo, A.H.S.; Faure, J. and Gerreira, J.M.F. An in vitro biological and antimactobial study on a sol-gewl derived silver-incorporated bioglass system. *Dental Materials*, 2008, 24, 1343-1351.

[17] Singh, D.; Bae, Y.; Singh, D.; Won, S.T.; Kim, J.H.; Han, S.S. Novel Chitosan-HEMA-Gelatin Macroporous Scaffold for Bone Tissue Engineering. *J. Biomater. Tissue Eng.* 2015, 5, 479-485.

[18] Aksoy, E.A.; Sezer, U.A.; Kara, F. and Hasirci, N. Heparin/Chitosan/Alginate Complex Scaffolds as Wound Dressings: Characterization and Antibacterial Study Against Staphylococcus epidermidis. *J. Biomater. Tissue Eng.* 2015, 5, 104-113.

[19] Alfano, A.L.; Fernandez, J.M. Induction of Topographical Changes in Poly- -Caprolactone Scaffolds for Bone Tissue Engineering: Biocompatibility and Cytotoxicity Evaluations. *J. Biomater. Tissue Eng.* 2015, 5, 142-149.

[20] Choudhury, M.; Mohanty, S. and Nayak, S. Effect of Different Solvents in Solvent Casting of Porous PLA Scaffolds-In Biomedical and Tissue Engineering Applications. *J. Biomater. Tissue Eng.* 2015, 5, 1-9.

[21] Gao, P.; Zhang, H.; Xiao, X.; Liu, Y.; Geng, L.; Yuan, Y.; Fan, B.; Liu, D.; Lian, Q.; Lu, J.; Wang, Z. An Innovative Osteo-Regenerator Based on Beta-Tricalcium Phosphate Granules for Bone Tissue Engineering. *J. Biomater. Tissue Eng.* 2015, 5, 50-55.

[22] Barba-Izquierdo, A. J. Salinas and M. Vallet-Regi. In vitro calcium phosphate layer formation on sol-gel glasses of the CaO-SiO2. *J. Biomed Mater. Res.* 47, 1000, 243-250.

[23] P. Saravanapavan, I.; Hench, L.L. Mesoporous calcium silicate glasses. I. Synthesis. *Journal of Non-Crystalline Solids*, 2003, 318, 1-13.

[24] Phulé, P.P.; Wood, T.E. *Ceramics and Glasses, Sol-Gel Synthesis, in Encyclopedia of Materials: Science and Technology*, 2001, 1090-1095, ISBN: 0-08-0431526.

[25] Julian, R. J.; Lisa, M. E.; Larry, L. H. Optimising bioactive glass scaffolds for bone tissue engineering. *Biomaterials*, 2006, 27, 7, 964-973.

[26] Balamurugan, A.; Sockalingum, G.; Michel, J.; Fauré, J.; Banchet, V.; Wortham, L.; Bouthors, S.; Laurent-Maquin, D.; Balossier. G. Synthesis and characterization of sol gel derived bioactive glass for biomedical applications. *Materials Letters*, 2006, 60, 3752-3757.

[27] Newport, R.J.; Skipper, L.J.; FitzGerald, V.; Pickup, D.M.; Smith, M.E. and Jones. J.R. In vitro changes in the structure of a bioactive calcia–silica sol–gel glass explored using isotopic substitution in neutron diffraction. *Journal of Non-Crystalline Solids*, 353 (2007), 1854-1859.

[28] Gupta, R.; Mozumdar, S.; Chaudhury, N.K. Fluorescence spectroscopic studies to characterize the internal environment of tetraethyl-orthosilicate derived sol–gel bulk and thin films with aging. *Biosensors and Bioelectronics*, 2005, 20(7), 1358-1365.

[29] Siriphannon, P.; Kameshima, Y.; Yasumori, A.; Okada, K.; Hayashi, S. Formation of hydroxyapatite on CaSiO3 powders in simulated body fluid. *Journal of the European Ceramic Society*, 2002, 22, 511-520.

[30] Drouet, C.R.C.; Sfihi, H.; Barroug, A. Physico-chemical properties of nanocrystalline apatites: Implications for biominerals and biomaterials. *Materials Science and Engineering C*, 2007, 27, 198-205.

[31] A. Meiszterics and K. Sink′o. Sol–gel derived calcium silicate ceramics. *Colloids and Surfaces A: Physicochem. Eng. Aspects*, 2007.

[32] Crayston, J.A. Sol-gel, Comprehensive Coordination Chemistry II. 2003, 1, 711-730, ISBN: 0-08-0443230.

[33] Alemany, M.I., Velasquez, P.; De la Casa-Lillo, M.A.; De Aza, P.N. Effect of materials processing methods on the in vitro bioactivity of wollastonite glass-ceramic materials. *Journal of Non-Crystalline Solids*, 2005, 351, 1716-1726.

[34] Lukito, D.; Xue, J.M.; Wang, J. In vitro bioactivity assessment of 70 (wt.) %SiO2–30 (wt.) %CaO bioactive glasses in simulated body fluid. *Materials Letters*, 2005, 59, 3267-3271.

[35] Olmo, N.; Ana, I.M.; Antonio, J.S.; Turnay, J.; Vallet-Reg, M.; Lizarbe, M.A. Bioactive sol–gel glasses with and without a hydroxycarbonate apatite layer as

substrates for osteoblast cell adhesion and proliferation. *Biomaterials*, 2003, 24, 3383-3393.

[36] Barba, I.; Conde, F.; Olmo, N.; Lizarbe, M.A.; Garc á, M.A.; Vallet-Reg í M. Vitreous SiO2–CaO coatings on Ti6Al4V alloys: Reactivity in simulated body fluid versus osteoblast cell culture. *Acta Biomaterialia*, 2006, 2, 4, 445-455.

[37] mila, A.R.; Vallet- Regm, M. Static and dynamic in vitro study of a sol-gel glass bioactivity. *Biomaterials*, 2001, 22, 2301-2306.

[38] Wei-hong, Z.; Jin-shu, C.; Jian, Q.; Xian-chun, L., Jian, L.I. Crystallization and properties of some CaO-A12O3-SiO2 system glass-ceramics with Y2O3 addition. *Trans. Nonferrous Met. SOC. China*. 2006, 16, 105-108.

[39] Xia, W. and Chang, J. Well-ordered mesoporous bioactive glasses (MBG): A promising bioactive drug delivery system. *Journal of Control Release*, 2006, 110, 3, 522-530.

[40] Brinker, C.J.; Scherer, G.W. The physics and chemistry of sol-gel processing. Achdemic Press Inc., San Diego, CA, USA, 1990.

[41] Lao, J.; Nedelec, J.M.; Moretto, Ph.; Jallot, E. Micro-PIXE characterization of interactions between a sol–gel derived bioactive glass and biological fluids. *Nuclear Instruments and Methods in Physics Research B*, 245 (2006), 511-518.

[42] Balamurugan, A.; Sockalingum, G.; Michel, J.; Faur é J.; Banchet, V.; Wortham, L.; Bouthors, S.; Laurent-Maquin, D.;; Balossier, G. Synthesis and characterization of sol gel derived bioactive glass for biomedical applications. *Materials Letters*, 2006, 60, 3752-3757.

[43] Liu, J. and Miao, X. Sol–gel derived bioglass as a coating material for porous alumina scaffold. *Ceramics International*, 2004, 30, 1781-1785.

[44] Wang, H.; Zhang, Q.; Yang, H. and Sun, H. Synthesis and microwave dielectric properties of CaSiO3 nanopowder by the sol–gel process. *Ceramics International*, 2008, 34, 1405-1408.

[45] Huang, Y.-B.; Lin, M.-W.; Liu, M.-Y.; Chen, C.-L. Composite of Decellular Adipose Tissue with Chitosan-Based Scaffold for Tissue Engineering with Adipose-Derived Stem Cells. *J. Biomater. Tissue Eng.* 2015, 5, 56-63.

[46] Nezafati, N.; Zamanian, A. Effect of Silane-Coupling Agent Concentration on Morphology and In Vitro Bioactivity of Gelatin-Based Nanofibrous Scaffolds Fabricated by Electrospinning Method. *J. Biomater. Tissue Eng.* 2015, 5, 78-86.

[47] Kim, K.; Kim, D.Y.; Baek, J.H.; Kim, J.H.; Park, Y.H.; Kim, Y.J.; Min, B.H.; Kim, M.S. Comparison of the In Vivo Bioactivity of Electrospun Poly(D,L-lactic-co-glycolic acid) and Poly(L-lactide) Fibrous Scaffolds. *J. Biomater. Tissue Eng.* 2015, 5, 372-377.

[48] Lao, J.; Nedelec, J.M.; Moretto, Ph. and Jallot, E. Biological activity of a SiO2–CaO–P2O5 sol–gel glass highlighted by PIXE–RBS methods. *Nuclear Instruments and Methods in Physics Research B*, 2007, 261, 488-493.

[49] Chen, Q.; Miyaji, F.; Kokubo, T. and Nakamura, T. Apatite formation on PDMS-modified CaO-SiO2-TiO2 hybrids prepared by sol-gel process. *Biomaterials*, 1999, 20, 1127-1132.

[50] Wang, E. and Chow, K.; Kwan, V.; Chin, T.; Wong, C. and Bocarsly, A. Fast and long term optical sensors for pH based on sol–gels. *Analytica Chimica Acta*, 2003, 495, 1-2, 45-50.

[51] Scherer, G.W. Structure and properties of gels. *Cem. Concr. Res.* 1999, 29(8), 1149-1157.

[52] Viitala, R.; Jokinen, M.; Peltola, T.; Gunnelius, K. and Rosenholm, J.B. Surface properties of in vitro bioactive and non-bioactive sol–gel derived materials. *Biomaterials*, 2002, 23, 3073-3086.

[53] Binnaz, A.; Hazar. Y. Preparation and in vitro bioactivity of $CaSiO_3$ powders. *Ceramics International*, 2007, 33, 687-692.

[54] Hayashi, Sh.; Nakagawa, Z.; Yasumori, A. and Okada, K. Effects of H2O in EtOH-H2O disperse medium on the electrophoretic deposition of $CaSiO_3$ Fine Powder. *Journal of the European Ceramic Society*, 1999, 19, 75-79.

[55] Padilla, S.; Román, J.; Carenas, A. and Vallet-Regì M. The influence of the phosphorus content on the bioactivity of sol–gel glass ceramics. *Biomaterials*, 2005, 26475-483.

[56] Long, L.H.; Chen, L.D. and Chang, J. Low temperature fabrication and characterizations of β-$CaSiO_3$ ceramics. *Ceramics International*, 32 (2006), 457-460.

[57] Lin, K.; Zhai, W.; Ni, S.; Chang, J.; Zeng, Y.; Qian. W. Study of the mechanical property and in vitro biocompatibility of CaSiO3 ceramics. *Ceramics International*, 2005, 31, 323-326.

[58] Long, L.H.; Chen, L.D.; Bai, S.Q.; Chang, J. and Lin. K.L. "Preparation of dense β-CaSiO3 ceramic with high mechanical strength and HAp formation ability in simulated body fluid". *Journal of the European Ceramic Society*, 2006, 26, 1701-1706.

[59] Haiyan, L. and Chang, J. Fabrication and characterization of bioactive wollastonite /PHBV composite scaffolds. *Biomaterials*, 2004, 25, 5473-5480.

[60] Meseguer-Olmo, L.; Bernabeu-Esclapez, A.; Ros-Martinez, E.; Sa′nchez-Salcedo, S.; Padilla, S.; Martìn, A.I.; Vallet-Regì M.; Clavel-Sainz, M.; Lopez-Prats, F.; Meseguer-Ortiz, C.L. In vitro behaviour of adult mesenchymal stem cells seeded on a bioactive glass ceramic in the SiO2–CaO–P2O5 system. *Acta Biomaterialia*, 2008, 4, 1104-1113.

[61] Lin, K.; Chang, J.; Zeng, Y.; Qian, W. Preparation of macroporous calcium silicate ceramics. *Materials Letters*, 2004, 58, 2109-2113.

[62] Wu, Ch.; Ramaswamy, Y.; Kwik, D.; Zreiqat, H. The effect of strontium incorporation into $CaSiO_3$ ceramics on their physical and biological properties. *Biomaterials*, 2007, 28, 3171-3181.

[63] Kokubo, T.; Kim, H.; Kawashita, M. Handbook of Advanced Ceramics. *Ceramics for Biomedical Applications*, 2003, 385-416, Chapter 14-14.1.

[64] Wan, X.; Hu, A.; Li, M.; Chang, Ch.; Mao, D. Performances of CaSiO3 ceramic sintered by Spark plasma sintering. *Materials Characterization*, 2008, 59, 256-260.

[65] Arstila, H.; Vedel, E.; Hupa, L. and Hupa, M. Factors affecting crystallization of bioactive glasses. *Journal of the European Ceramic Society*, 2007, 27, 1543-1546.

[66] Liu, X. and Ding, Ch. Characterization of plasma sprayed wollastonite powder and coatings. *Surface and Coatings Technology*, 2002, 153, 2, 173-177.

[67] Peng, F.; Liang, K.; Hu, A.; Shao, H. Nano-crystal glass-ceramics obtained by crystallization of vitrified coal fly ash. *Fuel*, 2004, 83, 14-15, 1973-1977.

[68] Yuvarani, I.; Senthilkumar, S.; Venkatesan, J.; Kim, S.; Al-Kheraif, A.A.; Anil, S.; Sudha, P.N. Chitosan Modified Alginate-Polyurethane Scaffold for Skeletal Muscle Tissue Engineering. *J. Biomater. Tissue Eng.* 2015, 5, 665-672.

[69] Jiang, X.; Wu, H.; Zheng, L.; Zhao, J. Effect of In-Situ Synthesized Nano-Hydroxyapatite/Collagen Composite Hydrogel on Osteoblasts Growth In Vitro. *J. Biomater. Tissue Eng.* 2015, 5, 523-531.

[70] Guo, W.; Han, L.; Xia, R.; Cui, F.; Chen, S.; Ma, J.; Pan, J. Repair of Mandibular Critical-Sized Defect of Minipig Using In Situ Periosteal Ossification Combined with Mineralized Collagen Scaffolds. *J. Biomater. Tissue Eng.* 2015, 5, 439-444.

[71] Venkatesan, J.; Jayakumar, R.; Anil, S.; Chalisserry, E.P.; Pallela, R.; Kim, S. Development of Alginate-Chitosan-Collagen Based Hydrogels for Tissue Engineering. *J. Biomater. Tissue Eng.* 2015, 5, 458-464.

[72] Wang, J.; Cheng, N.; Yang, Q.; Zhang, Z.; Zhang, Q.; Biomater, J. Double-Layered Collagen/Silk Fibroin Composite Scaffold That Incorporates TGF-ß1 Nanoparticles for Cartilage Tissue Engineering. *J. Biomater. Tissue Eng.* 2015, 5, 357-363.

[73] Wei, X.; He, K.; Yu, S.; Zhao, W.; Xing, G.; Liu, Y.; Sun, J. RGD Peptide-Modified Poly(lactide-co-glycolide)/ß-Tricalcium Phosphate Scaffolds Increase Bone Formation After Transplantation in a Rabbit Model. *J. Biomater. Tissue Eng.* 2015, 5, 378-386.

[74] Liu, J.; Mao, K.; Wang, X.; Guo, W.; Zhou, L.; Xu, J.; Liu, Z.; Mao, K.; Tang, P. Calcium Sulfate Hemihydrate/Mineralized Collagen for Bone Tissue Engineering: In Vitro Release and In Vivo Bone Regeneration Studies. *J. Biomater. Tissue Eng.* 2015, 5, 267-274.

[75] He, H.; Li, W.; Su, J.; Wang, H.; Ye, Z.; Cai, M.; Hou, B.; Liang, C.; Gong, J.; Guo, Y. In Vitro Evaluation of the Cytocompatibility of an Acellular Rat Brain Matrix Scaffold with Neural Stem Cells" *J. Biomater. Tissue Eng.* 2015, 5, 628-634.